JOURNAL OF THERMOPHYSICS AND HEAT TRANSFER
Vol. 20, No. 4, October–December 2006

Film Cooling Effectiveness of an Advanced-Louver Cooling Scheme for Gas Turbines

X. Z. Zhang* and I. Hassan†
Concordia University, Montréal, Québec H3G 1M8, Canada

DOI: 10.2514/1.18898

A novel film-cooling scheme for high temperature gas turbine applications was introduced in this paper. Compared with the traditional circular hole, the new scheme combines both the advantages of traditional film cooling with those of impingement cooling. The hole that transports coolant fluid from the inside to the outside of the blade is designed in such a way that the coolant must go through a bend before exiting the blade, thus impinging on the blade material. This scheme is expected to produce the greatest coverage on the blade with the least amount of mixing and least possible amount of coolant. A benchmark case of a traditional circular hole in a crossflow, the fundamental problem of film cooling, was employed to validate the present methodology with the jet liftoff effect clearly captured in the simulation. Turbulence was modeled using four different turbulence models, namely, k–ε (including its three variants), k–ω, Reynolds-stress, and Spalart–Allmaras with different wall treatments. It was found that the proposed cooling scheme can prevent the jets from penetrating into the mainstream much better and provide more uniform protection on the surface, indicating that the proposed scheme yields superior performance.

Nomenclature

DR	=	density ratio, ρ_j/ρ_∞
d	=	hydraulic diameter of hole, m
k	=	turbulent kinetic energy, m^2/s^2
L	=	length of injection hole (for cylindrical holes), m
m	=	blowing ratio, $\rho_j U_j/\rho_\infty U_\infty$
T	=	temperature, K
U	=	velocity, m/s
x	=	streamwise coordinate, m
y	=	vertical coordinate, m
y^+	=	nondimensional wall distance, $\rho u_\tau y_p/\mu$
z	=	spanwise coordinate, m
ε	=	dissipation rate of turbulent kinetic energy, m^2/s^3
η	=	local adiabatic film-cooling effectiveness, $(T_{aw} - T_\infty)/(T_j - T_\infty)$
ρ	=	density, kg/m^3

Subscripts and Superscripts

aw	=	adiabatic wall
j	=	refers to the jet
w	=	wall conditions
∞	=	mainstream conditions at inlet plane and in freestream

I. Introduction

MODERN gas turbine engines typically operate with inlet temperatures of 1800–2000 K, which is far beyond the allowable metal temperature. Film cooling is extensively used to provide protection for the metal against this severe thermal environment. Whereas a large amount of coolant provides better surface coverage downstream of the jets, using too much coolant, on the other hand, can incur a severe efficiency penalty. The designer's goal is to minimize the coolant consumption, maximize the cooling efficiency, and produce acceptable temperature and thermal stress levels on the turbine blade surface. Over the past decades, significant effort has been devoted to developing effective cooling strategies to maintain the blade temperature below the melting point of alloys used to construct the airfoils. As a result, various cooling strategies have been developed such as film, impingement, and multipass cooling.

Many experimental and computational studies have been conducted regarding the cooling process of gas turbine blades to understand the complex flow and heat transfer processes and to devise the best possible cooling schemes. Methods that have mainly been investigated include film cooling (Hyams and Leylek [1], Cho et al. [2], Gartshore et al. [3], Goldstein et al. [4], Cutbirth and Bogard [5], and Yuen and Martinez-Botas[6]), impingement cooling (Son et al. [7] and Taslim et al. [8]), and advanced internal or external cooling (Azad et al. [9] and Taslim et al. [8]). These methods are commonly studied along with the following parameters: injection orientations (Brittingham et al. [10], Jung et al. [11], Gritsch et al. [12], and Dittmar et al. [13]), hole length (Burd et al. [14] and Harrington et al. [15]), freestream turbulence (Ekkad et al. [16], Mayhew et al. [17], and Saumweber et al. [18]), hole entrance effects (Hale et al. [19], Wilfert and Wolff [20], and Gritsch et al. [21]), hole exit tapering (Kohli and Bogard [22] and Sargison et al. [23]), hole exit expanding (Gritsch et al. [21], York and Leylek [24], and Kim and Kim [25]), and density ratio effects (Ekkad et al. [16]). Only recent references have been given here, and earlier reports may be traced through the reference lists of the papers cited. From these reports, some broad generalizations can be made about the methods, geometries, and conditions most appropriate for internal or external cooling of gas turbine blades.

1) Hole geometry is an important parameter for film-cooling performance. Laterally and forward-expanded holes provide higher values of spanwise averaged effectiveness and lower values of spanwise averaged heat transfer coefficients than laterally expanded holes. Flared holes have the best overall performance, especially at high blowing ratios. Compound angle injection, whether for shaped or circular holes, leads to an increase in spanwise averaged effectiveness compared with that obtained with standard circular holes.

2) For standard circular holes on a flat surface with low mainstream turbulence intensities, the downstream effectiveness is optimum for blowing ratios of approximately 0.5. For blowing ratios above this value, the coolant jet undergoes liftoff. This allows the hot

Received 18 July 2005; revision received 12 December 2005; accepted for publication 3 February 2006.

*Department of Mechanical and Industrial Engineering.
†Department of Mechanical and Industrial Engineering; IbrahimH@me.concordia.ca

gases to come in contact with the surface, which causes the effectiveness to decrease. The jet liftoff effect is not captured at all in the predictions for the cylindrical hole scheme at high blowing ratios more than 0.5. This is attributed to many factors such as the deficiency of turbulence models, the use of isotropic eddy viscosity models, the presence of recirculation regions, as well as the use of wall functions.

3) Compound angle injection, whether for shaped or circular holes, leads to an increase in spanwise averaged effectiveness compared with that obtained with standard circular holes. However, compound jets generally produce higher heat transfer coefficients on the surface than do simple injection jets, and this trend is amplified as the blowing ratio rises. Hole spacing affects the ability of adjacent jets to coalesce. Small hole spacing results in better coverage of the wall, and thus higher effectiveness values as compared with larger ones. A pitch-to-diameter ratio of 3 was commonly used in film-cooling studies.

4) It is necessary to include the plenum and film hole in the computational domain to ensure a realistic profile at the exit of the jet, and to account for the interaction between the mainstream, the jet, and the plenum. All plenums with flow direction were observed to yield superior effectiveness compared with that for the standard stagnant plenum. The plenum flow direction has an effect on cooling effectiveness only when the plenum height is less than $2d$. Counterflow plenums produce better centerline effectiveness in the near-hole region than that in coflow plenums at low and high blowing ratios. However, at high blowing ratios, the coflow performs best in terms of spanwise averaged effectiveness for $x/d \geq 2$.

5) Different turbulence models have been applied to a variety of experimentally measured cases and the predictions vary significantly with different turbulence models. Of the several near-wall treatments, a two-layer wall treatment produced a more consistent solution than the standard wall or nonequilibrium wall functions. The higher order discretization scheme results in less numerical diffusion and yields more accurate results than the lower order scheme.

Few studies in the open literature have focused on novel cooling schemes for increased cooling performance. A comprehensive review of shaped holes was presented by Bunker [26] recently. To date, most film-cooling schemes aim to cool the turbine airfoil surface downstream of injection. With the new cooling concept, first designed by Immarigeon [27] in collaboration with Pratt & Whitney Canada and refined by the authors to show its full advantages, a greater portion of the airfoil is protected. This scheme combines both the advantages of traditional film cooling with those of impingement cooling. The film hole that transports coolant fluid from the inside to the outside of the blade is designed in such a way that the coolant must go through a bend before exiting the blade, thus impinging on the blade material. Finally, the flow exits very close to the blade surface, minimizing aerodynamic losses. The present study will also numerically investigate the capability of the current turbulence models to capture the right trend for adiabatic effectiveness. To justify the new methodology, systematic simulations have been performed on a benchmark case at different blowing ratios and density ratios. For the first time, to the best of authors' knowledge, the jet liftoff effect in traditional cylindrical holes is clearly captured in the simulations at high blowing ratios, and results are in excellent agreement with experimental data. The new methodology established in the benchmark case was applied to the new scheme.

II. Mathematical Modeling and Boundary Conditions

The computational domains and film-cooling geometries used in this study are shown in Figs. 1 and 2 for the Sinha et al. [28] case and the new scheme, respectively. Each domain consists of infinite rows of film-cooling holes on a flat plate, such that the end-wall effects can be neglected. The origin of the coordinate system was set at the trailing edge of the jet outlet. The parameters and the geometry in the present computational study were the same as in the experimental study. At the upstream inlet, a velocity inlet condition was applied with the free-stream turbulence being 0.2% as in the experimental work. At the outlet, a pressure boundary condition was applied. The

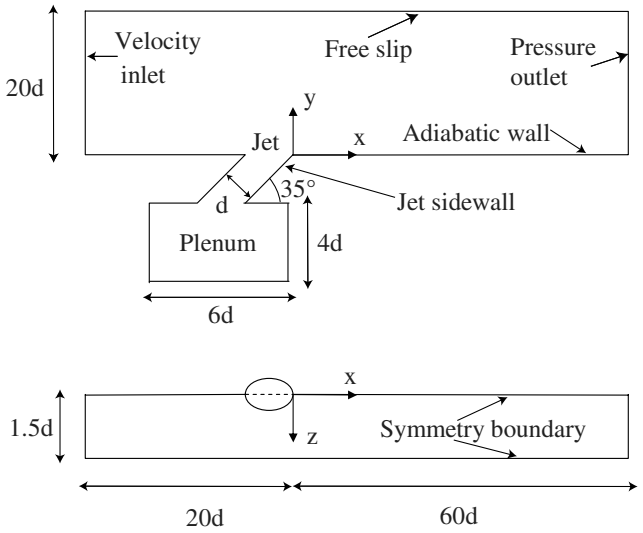

Fig. 1 Geometry and computational domain of a standard case, Sinha et al. [28].

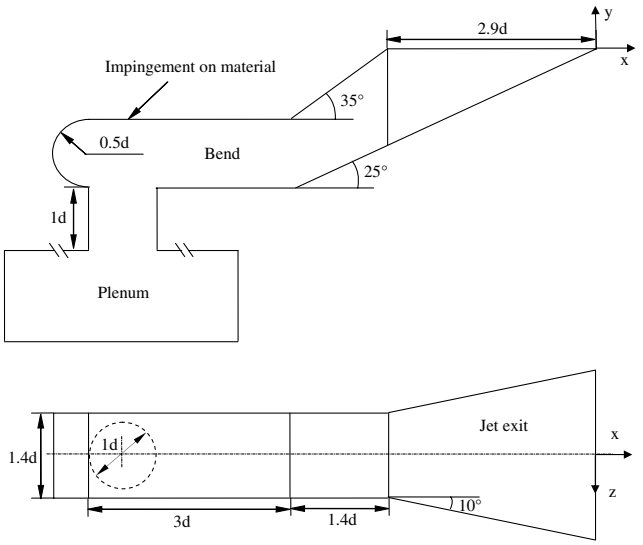

Fig. 2 Geometry of the jet section of the new scheme (same computational domain as Fig. 1).

domain extends $20d$ from the bottom test surface, far enough such that a free-slip boundary condition or zero shear stress may be applied. If the computational domain is symmetric about the central plane, symmetry boundary conditions are imposed at both the central plane and at the $1.5d$ plane in the streamwise direction. If the domain is asymmetric with a compound angle hole, a periodic boundary condition will be applied. At the bottom wall, as well as the other walls, an adiabatic wall boundary condition with no-slip was imposed. A typical mesh around the jet section for the new scheme is shown in Fig. 3.

In the present work, four turbulence models combined with different wall treatments were selected to perform the simulation by solving the Reynolds-averaged Navier–Stokes equations. The performances of these models, namely, the Spalart–Allmaras model, the k–ε model (including its three variants: standard k–ε, renormalization group (RNG) k–ε, and realizable k–ε), the k–ω model, and Reynolds-stress model, as well as the performance of different near-wall treatments, were evaluated. The predictions using these models were validated and compared with the experimental data obtained by Sinha et al. [28] and other researchers. It was found that the realizable k–ε model provided the most appropriate prediction of adiabatic film-cooling effectiveness both in the centerline and spanwise directions.

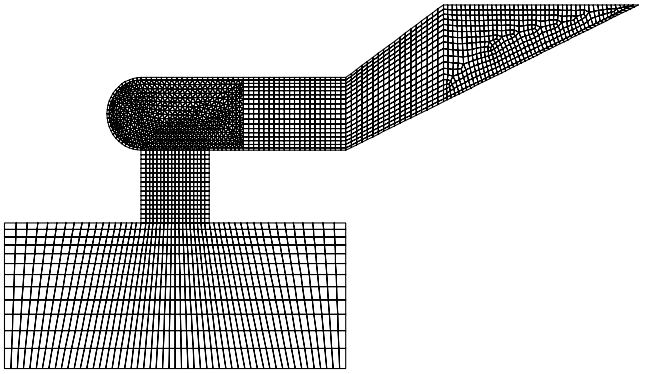

Fig. 3 Typical mesh in the jet section of the new scheme.

The CFD package FLUENT 6.0 is used to solve the Navier–Stokes equations. According to the experiments, it is assumed that the flow is incompressible, steady-state turbulent flow. The CFD package uses the finite volume method and supports unstructured grids. It enables the use of different discretization schemes and solution algorithms, together with various types of boundary conditions. As part of the same package, a preprocessor, Gambit, was used to generate the required grid for the solver. Different meshes were used at the beginning to determine the optimum grid size and to ensure a grid independent solution. The grid contained between 0.3 and 0.9×10^6 cells when wall functions were employed. When the enhanced wall treatment was selected, a grid independent solution was attained with a grid containing 1.6×10^6 cells. In this study, the hexahedral elements were mostly used with a multiblock structured mesh and tetrahedrons were used only when the subgeometries became very complex. Extremely strict convergence criteria were imposed, where at least 500 additional iterations were performed after the residuals leveled off. Both mass and energy were conserved throughout the domain. Convergence is determined when the difference between the mass in and mass out is less than 0.001% and when the energy imbalance is less than 0.02%.

III. Results and Discussion

In the present study, the experimental work of Sinha et al. [28] was chosen as the benchmark case to validate the methodology that was used in the new scheme. Additionally, it was selected to validate the selected turbulence models. There are a number of reasons in choosing this case to benchmark the numerical results. First of all, Sinha et al's case is a short cylindrical hole with a plenum, close to the real turbine blades applications. The computational domain has to include the plenum to accurately simulate the coupling dynamics of the flow between the mainstream, jet and plenum. Secondly, the material of the testing plate of Sinha et al.'s case is styrofoam with very low thermal conductivity ($0.027\ \mathrm{W/m \cdot K}$). This is considerably lower than the previous testing plate and can significantly reduce conduction error. In many efforts by different researchers, the heat conduction in the substrate has not been considered and their experimental results varied from one another to the extent that the difference could not be explained by measurement uncertainty alone. Thirdly, a cylindrical hole on a flat plate is the most fundamental problem in film cooling and has been studied extensively both experimentally and numerically. Although it is the simplest cooling scheme, satisfactory numerical prediction is notoriously difficult to obtain, particularly at a high blowing ratio. Nevertheless, the problem of a circular jet on a flat plate has to be solved satisfactorily before going to the next step, either simulating shaped holes or compound angle holes or both. Finally, since the publication of Sinha et al.'s experimental data, many researchers have kept trying with some success in improving the numerical results, such as Leylek and Zerkle [29], Mulugeta and Patankar [30], Leitner [31], Ferguson et al. [32], Walters and Leylek [33], Kapadia and Roy [34], and Immarigeon [27]. Therefore, this is a classic case in the arena of the film-cooling simulation.

As mentioned, Sinha et al. [28] has been compared with numerical predictions by many researchers over the years. All these papers documented that at a low blowing ratio of less than 0.5, their prediction agreed well with the experimental data. However, at a higher blowing ratio such as 1, the most significant disagreement occurred immediately downstream of the jet exit, with an error as much as 100%, as shown in Fig. 4. At a higher blowing ratio, the jets will lift off from the surface and penetrate into the main stream, causing the deterioration of protection. Most of the previous work, as far as the authors know, failed one way or another to capture the jet liftoff effect and this was attributed to either the deficiency of the turbulence models, the use of isotropic eddy viscosity models, the presence of a recirculation region, or the use of wall functions. It is interesting to note that in the literature, the separation and recirculation phenomenon of the flow immediately downstream of the injection was captured very well in terms of velocity vectors. However, in terms of temperature, adiabatic effectiveness, the jet liftoff effect has not been captured very well. Only after the jet liftoff effect in the traditional cylindrical hole scheme is captured satisfactorily in the numerical results can a parametric study of a new cooling scheme be done with confidence.

In the present study, a structured mesh was used rather than an unstructured one as was used in most recent publications. The first trial mesh was created with 50×10^3 cells and tested. From the solution of this first mesh the turbulence properties, such as the y^+ value, were checked to determine if a finer or coarser mesh close to walls and hole area was required to resolve the boundary layer appropriately according to the near-wall mesh requirements. The areas with large gradients, such as temperature or velocity, were also found from the test case. The size of the mesh was increased at least

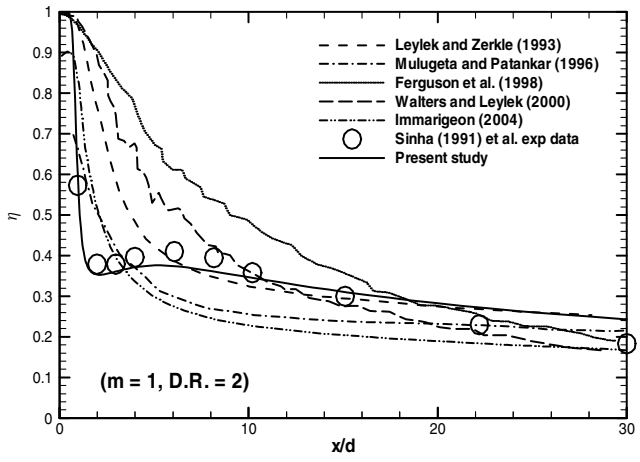

Fig. 4 Present and previous predictions for Sinha et al. [28] experimental data.

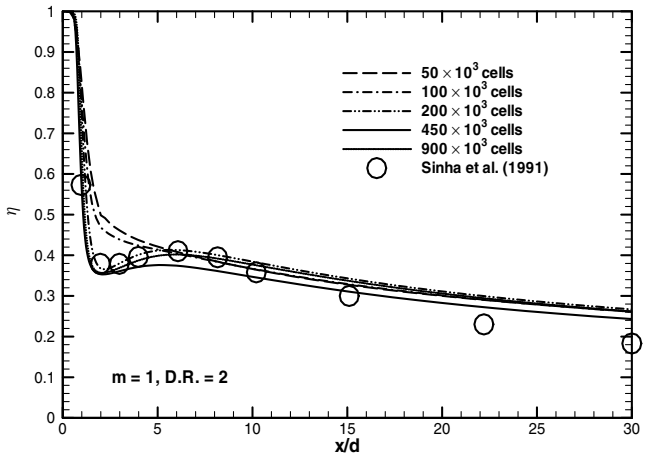

Fig. 5 Grid independence.

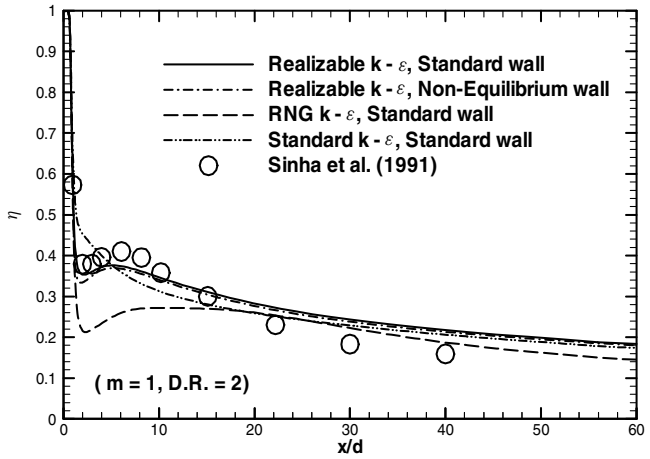

Fig. 6 The performance of the three variants of the k–ε model.

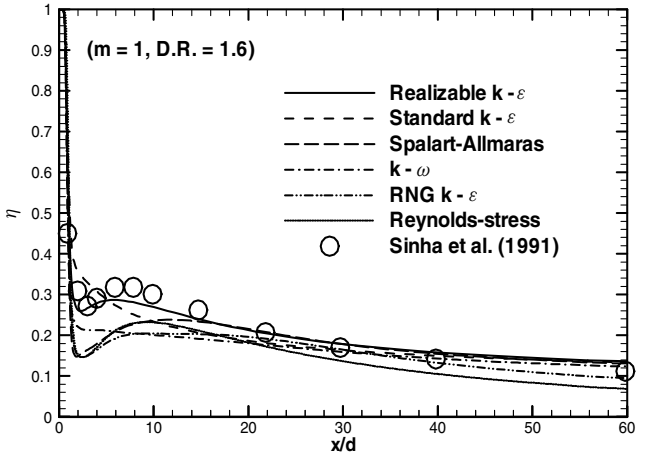

Fig. 7 The performance of turbulence models with the experimental data of Sinha et al. [28].

twice subsequently with the most grids concentrated in the large gradient areas and near the walls. After the second case was solved, the plot of a parameter of interest, for instance, adiabatic film-cooling effectiveness along the center line on the test wall, was compared with that of the first case. Chances are that the first two plots will not be very similar, although the results of the first two cases are close as shown in the Fig. 5. The reason for this is simply because the features of this flow were known beforehand. The size of the mesh continued to be increased following the same procedure until a point was reached such that further increasing the size of the mesh did not result in any significant change in the final parameter monitored. Figure 5 shows that to capture the fine features of the jet liftoff effect, a mesh has to have at least 200×10^3 cells. Although more cells may lead to a better solution the computing time increases exponentially. A mesh between 300×10^3 and 600×10^3 cells is appropriate to reach acceptable accuracy with a reasonable running time. It is of interest to note that the quality of the prediction with structured hexahedral elements of only 100×10^3 cells, dash-dot line in Fig. 5, is even better than that of Immarigeon [27] using unstructured tetrahedral elements of 800×10^3 cells, dash-dot-dot line shown in Fig. 4, indicating considerable economical advantage of the structured mesh.

Figure 6 shows the comparison between the experimental data and the prediction of centerline effectiveness at DR $= 2$ and $m = 1$, as well as the relative performance of the three variants of the k–ε models. The realizable k–ε model yielded a result the closest to the experimental data. The standard k–ε model completely missed the jet liftoff effect for this geometry. The RNG k–ε model considerably underpredicted the effectiveness in the near-hole region, although it did capture the jet liftoff. The figure also shows that the results for the nonequilibrium wall functions option are almost identical to that of the standard wall functions.

Figure 7 shows the performance of different turbulence models at DR $= 1.6$ and $m = 1$. Again, the realizable k–ε model outperformed all the other turbulence models. The standard k–ε missed the jet liftoff effect completely, whereas the k–ω model barely captures it. The RNG k–ε, Spalart–Allmaras, and Reynolds-stress models all significantly underpredicted the effectiveness in the near-hole region from $x/d = 2$ to 12, although all turbulence models captured the correct trend. At DR $= 1.6$ and $m = 0.9$ and DR $= 1.2$ and $m = 0.78$, excellent agreement between the experimental data and the predictions was obtained with the jet liftoff unquestionably

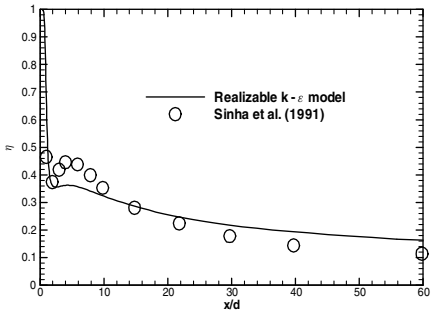

a) m = 0.9, D.R. = 1.6

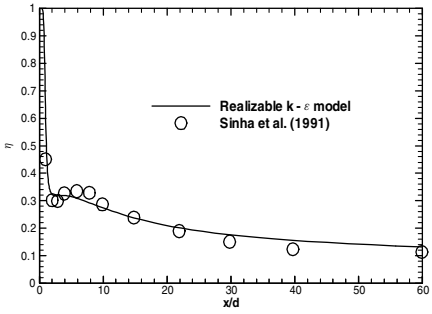

b) m = 0.78, D.R. = 1.2

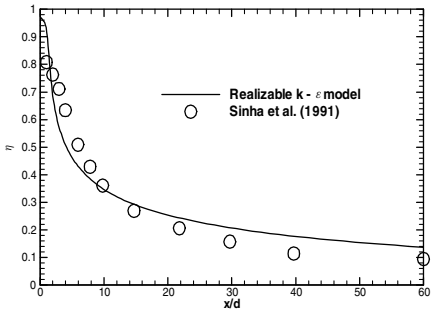

c) m = 0.5, D.R. = 1.2

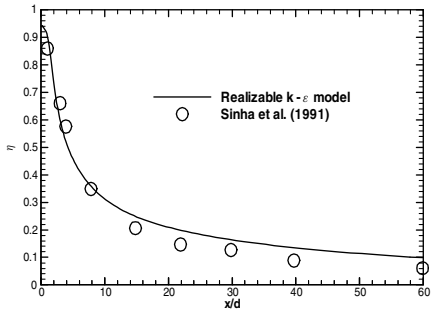

d) m = 0.25, D.R. = 1.2

Fig. 8 Predictions of η at different cooling parameters.

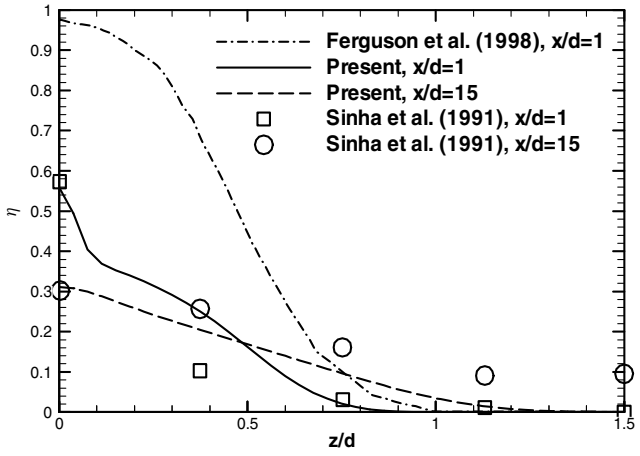

a) m = 1, D.R. = 2

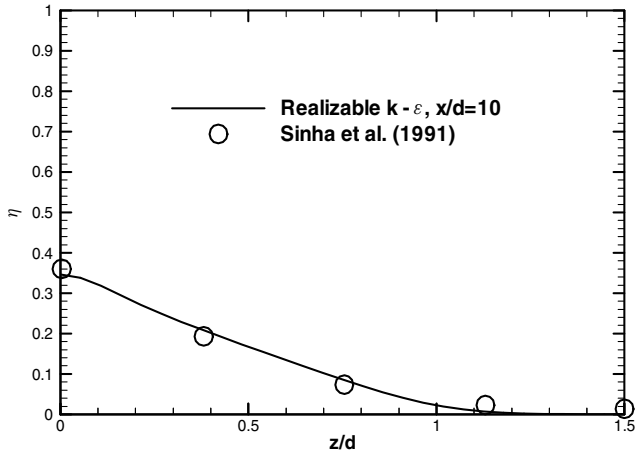

b) m = 0.5, D.R. = 1.2

Fig. 9 Predictions of η in the spanwise direction at different blowing ratios.

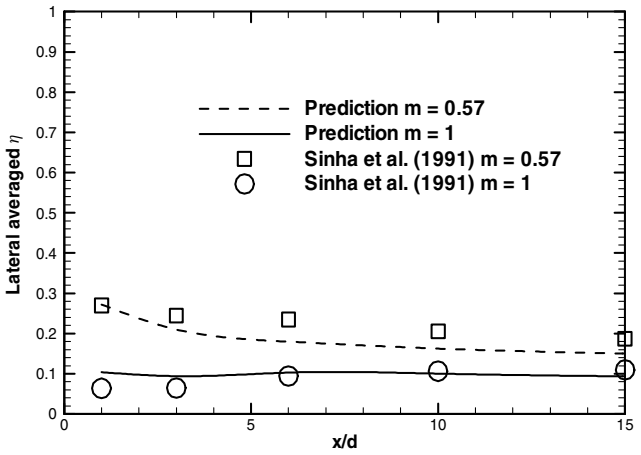

a) D.R. = 1.6

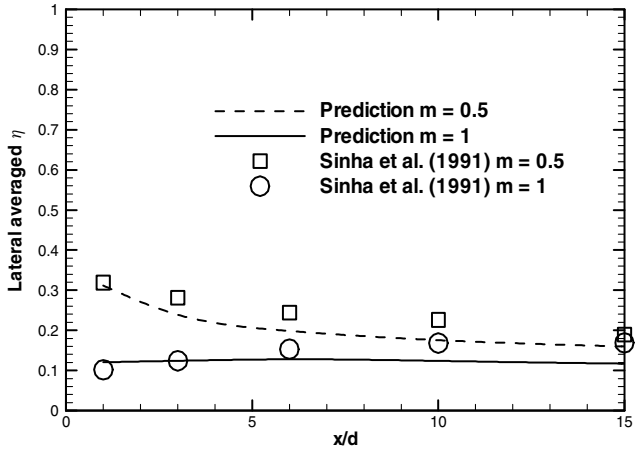

b) D.R. = 2

Fig. 10 Lateral averaged effectiveness at different blowing ratios.

captured, as shown in Figs. 8a and 8b. At lower blowing ratios of $m = 0.5$ and $m = 0.25$ with DR $= 1.2$ for both, the jets remained attached to the surface, and the agreement is shown in Figs. 8c and 8d.

Figure 9 shows the local effectiveness in the spanwise direction. The prediction agreed very well with the experimental data. The popular thought is that the current turbulence models systematically underpredict the adiabatic effectiveness in the spanwise direction. However, it seems the prediction would match the experimental data better if conduction error on the testing surface was taken into account in the experimental work, which to date has been neglected. Therefore, if the current turbulence models did underpredict the adiabatic effectiveness in the spanwise direction, the underprediction is not as severe as previously thought as long as all experimental error was taken into account, as confirmed by the predictions of lateral averaged effectiveness shown in Fig. 10.

The Sinha et al. [28] case confirms that the present methodology is fully capable of capturing the jet liftoff effect and can consistently give accurate results with density ratio ranging from 1.2 to 2.0 and blowing ratio ranging from 0.25 to 1.0, both in the centerline and in the spanwise direction. The possible reasons of capturing this correct trend are given next.

1) Structured meshes perform better than their unstructured counterparts. Recent researchers have favored unstructured meshes typically with tetrahedral elements. This is due to the fact that they are easy to generate and can be easily adapted to concentrate more nodes in areas of large gradients, as well as adjust the near-wall mesh according to the value of y^+. However, it is extremely difficult to control the distribution of the nodes and the truncation error is considerably larger than that of the hexahedral mesh. As a result, a large percentage of the nodes are placed in areas with small gradients resulting in unnecessarily fine meshes. Consequently, in the near-hole and wall regions the mesh is too coarse to resolve the wake of recirculation and boundary layers. The structured mesh (hexahedral elements, more efficient to fill the volume comparing to tetrahedron) on the other hand, is more difficult to create and cannot be adapted. Thus, if the y^+ is not appropriate to meet the near-wall mesh requirements, the mesh must be discarded and a new one created. However, the high fidelity of the solution and the high accuracy of a structured mesh is incomparable, and worth the extra effort. Figure 11 shows the comparison between the predictions given by structured and unstructured meshes. In these two cases the y^+ values are kept the same for all the walls in the domain. Apparently, the prediction of unstructured mesh with 740×10^3 cells failed to capture the jet liftoff effect although the unstructured mesh has more than three times more cells than the structured one, only 220×10^3 cells, with the same computational domain. Based on this study, to show the liftoff effect in the prediction using an unstructured mesh, the same quality of prediction as that of structured mesh shown in Fig. 11 requires at least 4×10^6 cells.

2) The y^+ issue has to be taken seriously. The present Reynolds-averaged turbulence models are empirical or semi-empirical and for the most part are only valid in the turbulence core flow far away from the boundary layer. Within the boundary layer, which has an extremely significant effect on the final solution, the current turbulence models unfortunately are not valid due to the presence of a laminar sublayer. Therefore, a series of empirical relations are brought in to bridge the gap between the fully developed turbulent core flow and

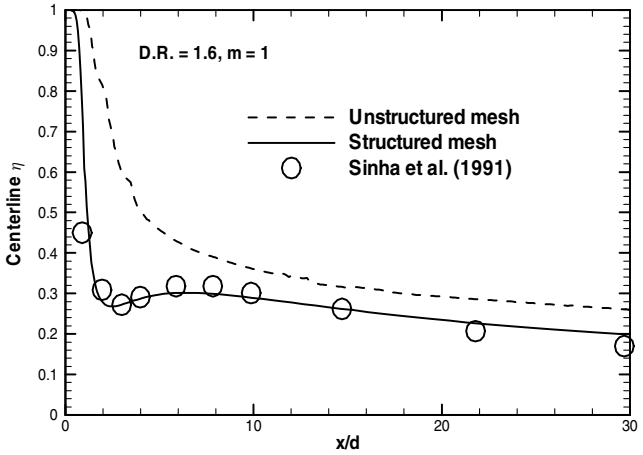

Fig. 11 Comparison between the predictions of structured and unstructured meshes.

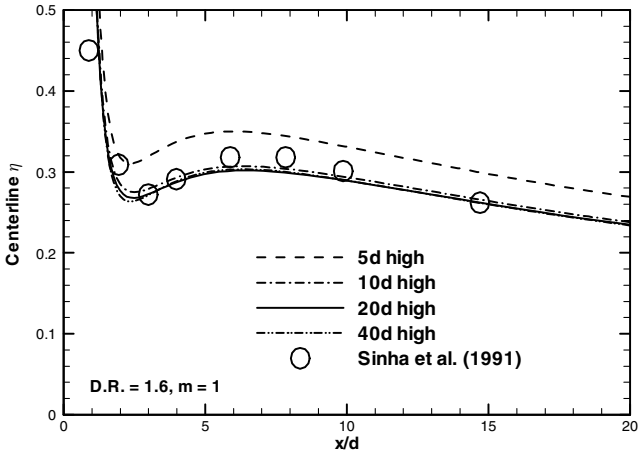

Fig. 12 The effect of the height of the duct section on the predictions.

the wall to reach closure. Hence, in order for the solution to be physically meaningful a certain requirement, namely, y^+, has to be satisfied. Wall functions have been validated over a wide range of y^+ values, so the near-wall mesh requirements are different depending on which code or commercial software is used. Even the two-layer zonal model approach, supposed to be able to resolve the laminar sublayer all the way to the wall, is also a set of empirical correlations with some near-wall mesh requirements attached. As long as all the near-wall mesh requirements are satisfied, the final solutions from different codes or softwares should be very close to each other. In this study, the value of y^+ falls into the range of 30 to 60 when standard wall functions are employed and on the order of 1 when enhanced wall treatment is selected, as dictated by the software FLUENT.

3) The selection of the computational domain is very important. During the course of the present study the selection of the height of the duct section of the computational domain definitely has some effect on the final solution. Because a height of $10d$ did not seem sufficient, different height values were tested, and it was found that $5d$ high is definitely too small and the results given by 20 and $40d$ high geometry were identical, as shown in Fig. 12. Kim and Benson [35] selected $7.5d$ high, Tyagi and Acharya [36] $5d$ high, Hale [37] $6d$, and Hoda et al. [38] $5d$, whereas most of the others selected $10d$ high in their benchmark studies in the open literature. This can partly explain the large discrepancies between the experimental data and their predictions in the immediate near-hole region. As in the Sinha et al. [28] study, the test was conducted in a wind tunnel with the test section of $0.6 \times 0.6 \times 2.4$ m by which the height is $47d$. The computational domain does not necessarily have to be exactly the same as in the experimental work; but in the computational study if the height of the duct is too small when the free-slip or zero shear stress boundary condition is imposed on the top wall of the duct, the flow will be squeezed hard in the vertical direction. Therefore, much less coolant will be able to penetrate into the mainstream during simulation than the coolant will do in the actual experiment. Consequently the effectiveness was significantly overpredicted and their evaluation of the performance of turbulence models was flawed.

In the benchmark case, the prediction compares very well with the experimental data. Using the present methodology, the realizable k–ε model consistently gives accurate results when different density ratios and different blowing ratios were considered. Thus, in the new scheme, the realizable k–ε model was selected to perform the simulations.

Figure 13a shows the centerline effectiveness at $m = 1$ and DR $=$ 2 for the new scheme. In the Sinha et al. [28] case, the jets lift off from the surface causing a sharp drop in effectiveness immediately downstream of injection. However, in the new scheme the jets remain attached to the surface and the effectiveness gradually decreases in the streamwise direction due to the fact that the bend redirects the flow from the vertical to horizontal direction, and that the increased cross-sectional area of the jets significantly reduces the momentum of the coolant. The effectiveness in the new scheme is substantially higher than that of the cylindrical hole. Also shown is the experimental data of forward and lateral shaped holes by Yu et al. [39]; see Fig. 14b for the hole geometry. The experimental data of Yu et al., with much lower effectiveness than that of the new scheme, have similar trend as that of the new scheme because in both cases the coolant did not lift off the surface. Figure 13b shows the centerline effectiveness at a blowing ratio of 0.5; the traditional cylindrical jets remain attached to the surface. Consequently, the centerline effectiveness is at the same level for both the traditional cylindrical jets

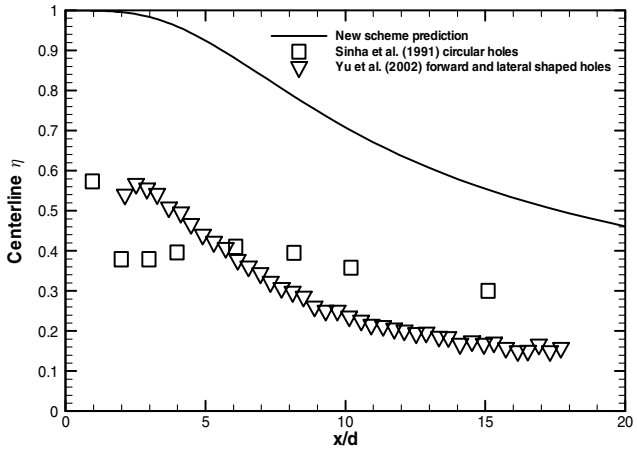

a) D.R. = 2, m = 1

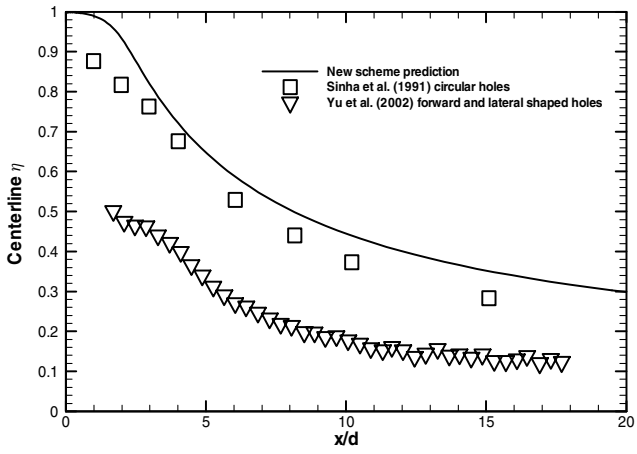

b) D.R. = 2, m = 0.5

Fig. 13 Centerline effectiveness of the new scheme.

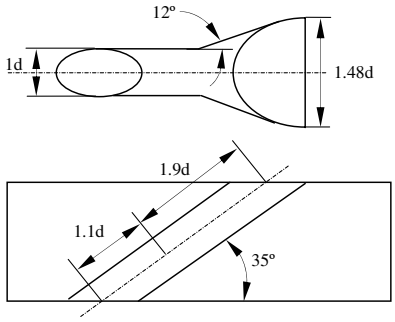

a) Bell et al. (2000)

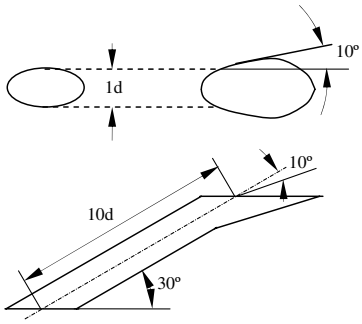

b) Yu et al. (2002)

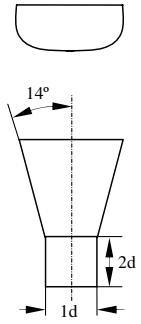

c) Dittmar et al. (2003)

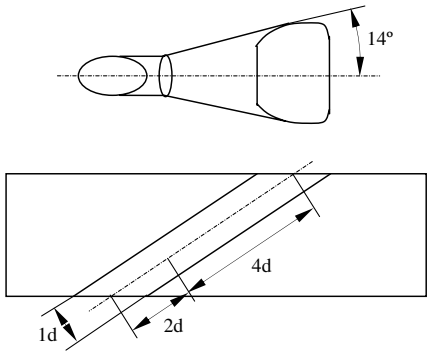

d) Saumweber et al. (2003)

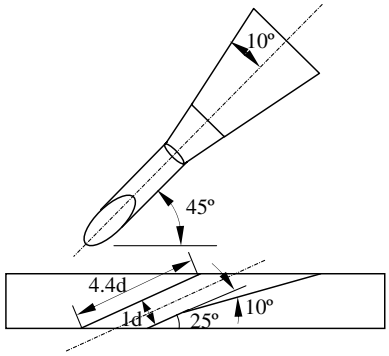

e) Taslim et al. (2005)

Fig. 14 Different cooling geometries (reproduced here) studied by researchers.

and the new scheme despite the fact that the coolant is stretched thin with the new scheme in the spanwise direction after injection.

Figure 15 shows the comparison of lateral averaged adiabatic effectiveness between different cooling schemes, namely, traditional circular holes by Sinha et al. [28], forward diffused holes by Bell et al. [40], both forward and lateral shaped holes by Yu et al. [39], straight fan-shaped holes by Dittmar et al. [13], fan-shaped holes by Saumweber et al. [18], and forward-lateral-diffused holes by Taslim et al. [41]. The geometries of these works are presented in Fig. 14. The new scheme yields the highest lateral averaged effectiveness, even at low blowing ratios below 0.5, when the jets in all schemes including the traditional cylindrical holes remain attached to the protected surface, as shown in Fig. 15a. The advantages of the new scheme are more evident at the higher blowing ratios above 1 when some cooling schemes such as circular holes undergo liftoff, as shown in Fig. 15b. As the coolant enters the bend, its momentum is reduced immediately as the cross-section of the flow path experiences a sudden increase. The bend then converts the momentum of the coolant from the vertical to horizontal direction. Further downstream towards the exit, the area of flow path increases gradually until the exit, further reducing the coolant momentum and enlarging the coverage area. All these factors contribute to the enhanced protection of the surface.

Figures 16 and 17 show the streamlines and the velocities of the two cooling schemes, namely, the circular hole and the new scheme, on the central plane at blowing ratio of 1 and density ratio of 2. From Fig. 16a the jet of the circular hole clearly lifts off the protected surface, penetrating into the mainstream. Figure 17a also shows the jet separation and recirculation after the injection in the circular jet scheme. Superimposed on the velocity vectors is the velocity contour. Figures 16b and 17b show the coolant in the new scheme stays close to the surface after exiting the hole without flow separation and recirculation. This indicates that the coolant in the new scheme provides less disturbing to the mainstream than the coolant in the circular jets does due to the reduced momentum and flared exit. The adiabatic effectiveness distribution in the spanwise direction is presented in Fig. 18. Along the $x/d = 1$ line, from $z/d = 0$ to 1, the local effectiveness of the new scheme is almost constant around 1, the highest possible value in effectiveness, much higher than that of the traditional cylindrical holes. Further downstream after the injection at $x/d = 15$, the effectiveness of the new scheme is still twice as high as that of the circular jets. Moreover, the effectiveness of the

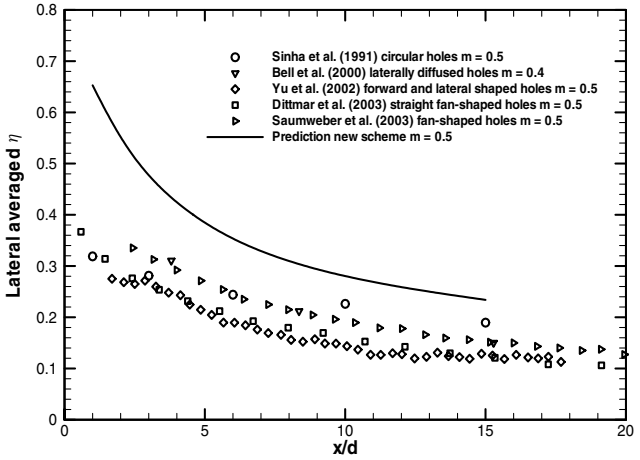

a) Low blowing ratio

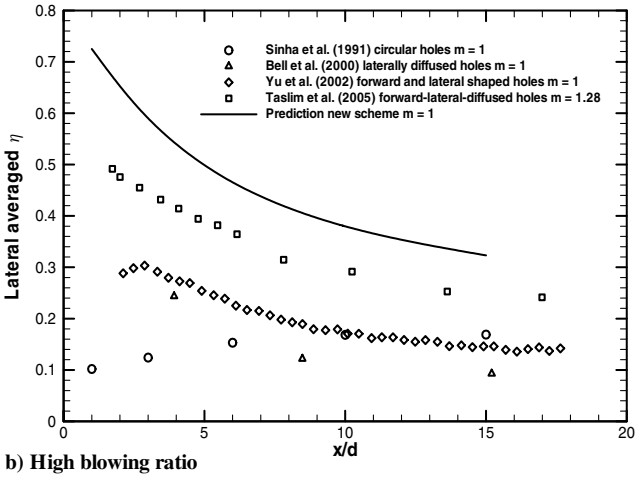

b) High blowing ratio

Fig. 15 Comparison of lateral averaged effectiveness between new scheme and different cooling schemes.

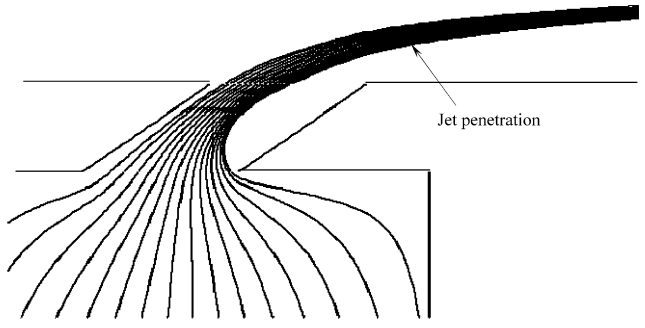

a) Circular hole

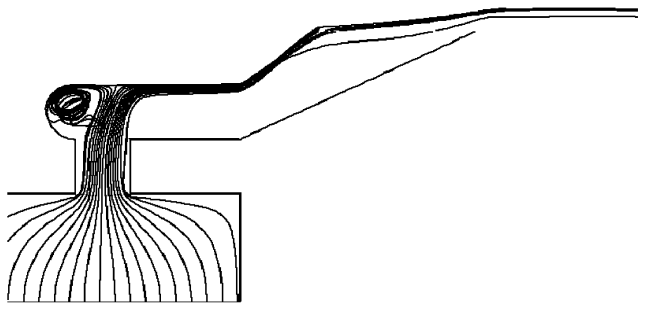

b) The new scheme

Fig. 16 Streamlines for different schemes on the central plane.

new scheme is more uniform than that of the traditional cylindrical jets.

For the two cases, both at $m = 1$ and 0.5, the new scheme gives more uniform effectiveness than the traditional cylindrical hole, especially at higher blowing ratios because the traditional cylindrical jet lifts off from the surface. Thus the new scheme will efficiently eliminate the presence of hot or cold spots on the protected surface, and significantly reduce thermal stress level on the turbine blade and elongate the expected service life of the engine. In the new scheme, the coolant remains attached to the surface for all blowing ratios tested from 0.5, 1, 3, 6, to 20, and even at 50. However, at a blowing ratio of 50, the velocity in the jet cross-section becomes supersonic. As a result, the incompressible assumption ceases to be valid. Thus, the simulation at blowing ratio of 50 has no physical meaning except for the purpose of showing whether or not the jets will lift off. With this new scheme, no matter how high the blowing ratio, the

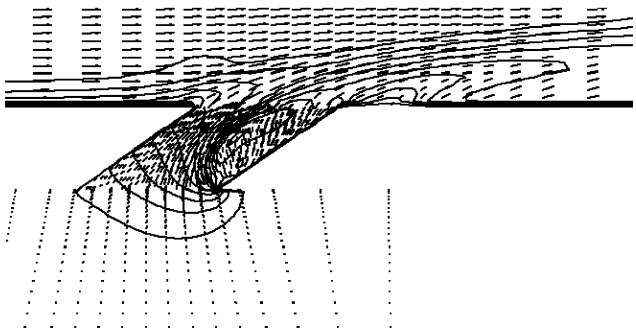

a) Circular hole

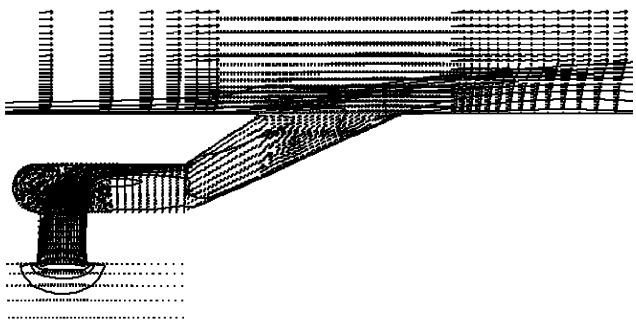

b) The new scheme

Fig. 17 Velocity vectors and contours for different schemes on the central plane.

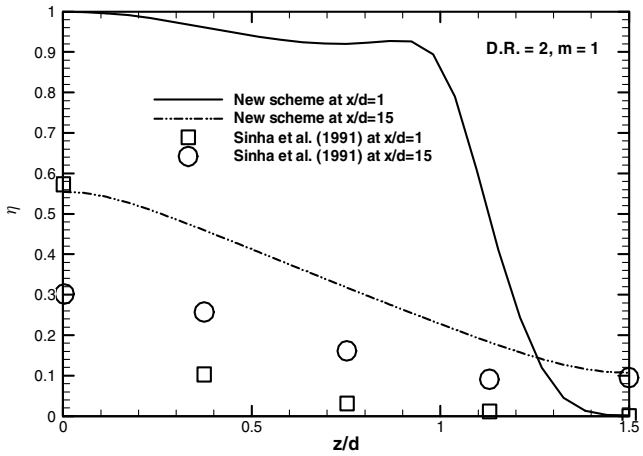

Fig. 18 Comparison of local effectiveness for new scheme with standard scheme of Sinha et al. [28].

possibility of jet liftoff is avoided, which will significantly reduce the disturbance to the mainstream and reduce the efficiency penalty. The only drawback is that as the coolant is stretched thinner in the spanwise direction after injection, the coolant has more surface area directly in contact with the hot mainstream when compared with the traditional cylindrical hole. Therefore, it is possible that more coolant could dissipate into the hot mainstream, which will reduce the protection slightly.

IV. Conclusions

In the present study, the performance of different turbulence models has been evaluated. Simulations of a benchmark case have been performed and excellent agreement between the predictions and available experimental data has been shown. The methodology, fully established in the benchmark simulations, was applied to a novel cooling scheme and its results are compared with some other cooling schemes including the cylindrical holes and some shaped holes. The new scheme combines in-hole impingement cooling with traditional downstream film-cooling for improved cooling capabilities. It was determined that the proposed cooling scheme can prevent coolant liftoff much better than standard round holes. The performance related to the heat transfer coefficient is a prospective topic for future studies. In particular, the heat transfer characteristics of the impingement jet inside the hole have an effect on the temperature of the target wall, thus influencing the performance of this cooling scheme overall. The key conclusions drawn from this study are

1) The jet liftoff effect in traditional cylindrical holes can be captured by current turbulence models when a high-quality mesh system is applied. The effect of near-wall mesh is significant because it demonstrates more effects on the final solution than the turbulence model and wall treatment combined.

2) The proposed cooling scheme can eliminate the possibility of jet liftoff and provide more uniform protection over the surface. It can considerably reduce the presence of hot spots in the blade and significantly reduce thermal stress.

The results presented in this work provide important insights for future computational studies of film cooling. Before this study, it was commonly believed that the current turbulence models were not capable of capturing the jet liftoff effect in the traditional cylindrical hole scheme, which is the most fundamental problem of film cooling and has been studied extensively in the open literature. Turbulence models and the quality of the numerical grid have a tremendous effect on the final solution. The quality of the mesh has such a big role in determining the solution that the performance of turbulence models could be completely masked. As a result, a poor quality mesh could accidentally produce excellent results. Thus, CFD practitioners must make sure that consistent results be obtained before drawing any conclusion. It is entirely possible that the current turbulence models have been unfairly blamed for not being able to predict some phenomena, when in reality they are if the model is set up properly.

References

[1] Hyams, D. G., and Leylek, J. H., "A Detailed Analysis of Film Cooling Physics: Part 3-Streamwise Injection with Shaped Holes," *Journal of Turbomachinery*, Vol. 122, No. 1, 2000, pp. 122–132.

[2] Cho, H. H., Rhee, D. H., and Kim, B. G., "Enhancement of Film Cooling Performance Using a Shaped Film Cooling Hole with Compound Angle Injection," *JSME International Journal, Series B (Fluids and Thermal Engineering)*, Vol. 44, No. 1, 2001, pp. 99–110.

[3] Gartshore, I., Salcudean, M., and Hassan, I., "Film Cooling Injection Hole Geometry: Hole Shape Comparison for Compound Cooling Orientation," *AIAA Journal*, Vol. 39, No. 8, 2001, pp. 1493–1499.

[4] Goldstein, R. J., and Jin, P., "Film Cooling Downstream of a Row of Discrete Holes With Compound Angle," *Journal of Turbomachinery*, Vol. 123, No. 2, 2001, pp. 222–230.

[5] Cutbirth, J. M., and Bogard, D. G., "Thermal Field and Flow Visualization Within the Stagnation Region of a Film-Cooled Turbine Vane," *Journal of Turbomachinery*, Vol. 124, No. 2, 2002, pp. 200–206.

[6] Yuen, C. H. N., and Martinez-Botas, R. F., "Film Cooling Characteristics of a Single Round Hole at Various Streamwise Angles in a Crossflow: Part 1 Effectiveness," *International Journal of Heat and Mass Transfer*, Vol. 46, No. 2, 2003, pp. 221–235.

[7] Son, C., Gillespie, D., Ireland, P., and Dailey, G., "Heat Transfer and Flow Characteristics of an Engine Representative Impingement Cooling System," *Journal of Turbomachinery*, Vol. 123, No. 1, 2001, pp. 154–160.

[8] Taslim, M. E., Setayeshgar, L., and Spring, S. D., "An Experimental Evaluation of Advanced Leading Edge Impingement Cooling Concepts," *Journal of Turbomachinery*, Vol. 123, No. 1, 2001, pp. 147–153.

[9] Azad, G. S., Han, J. C., Teng, S., and Boyle, R., "Heat Transfer and Pressure Distributions on a Gas Turbine Blade Tip," *Journal of Turbomachinery*, Vol. 122, Oct. 2000, pp. 717–724.

[10] Brittingham, R. A., and Leylek, J. H., "A Detailed Analysis of Film Cooling Physics: Part 4—Compound-Angle Injection With Shaped Holes," *Journal of Turbomachinery*, Vol. 122, Jan. 2000, pp. 133–145.

[11] Jung, I. S., and Lee, J. S., "Effects of Orientation Angles on Film Cooling over a Flat Plate: Boundary Layer Temperature Distributions and Adiabatic Film Cooling Effectiveness," *Journal of Turbomachinery*, Vol. 122, Jan. 2000, pp. 153–160.

[12] Gritsch, M., Schulz, A., and Wittig, S., "Effect of Crossflows on the Discharge Coefficient of Film Cooling Holes with Varying Angles of Inclination and Orientation," *Journal of Turbomachinery*, Vol. 123, No. 4, 2001, pp. 781–787.

[13] Dittmar, J., Schulz, A., and Wittig, S. "Assessment of Various Film-Cooling Configurations Including Shaped and Compound Angle Holes Based on Large-Scale Experiments," *Journal of Turbomachinery*, Vol. 125, No. 1, 2003, pp. 57–64.

[14] Burd, S. W., Kaszeta, R. W., and Simon, T. W., "Measurements in Film Cooling Flows: Hole L/D and Turbulence Intensity," *Journal of Turbomachinery*, Vol. 120, No. 4, 1998, pp. 791–798.

[15] Harrington, M. K., McWaters, M. A., Bogard, D. G., Lemmon, C. A., and Thole, K. A., "Full-Coverage Film Cooling With Short Normal Injection Holes," *Journal of Turbomachinery*, Vol. 123, No. 4, 2001, pp. 798–805.

[16] Ekkad, S. V., Han, J. C., and Du, H., "Detailed Film Cooling Measurements on a Cylindrical Leading Edge Model: Effect of Free-Stream Turbulence and Coolant Density," *Journal of Turbomachinery*, Vol. 120, No. 4, 1998, pp. 799–807.

[17] Mayhew, J. E., Baughn, J. W., and Byerley, A. R., "The Effects of Free-Stream Turbulence on Film Cooling Adiabtaic Effectiveness," *International Journal of Heat and Fluid Flow*, Vol. 24, No. 5, 2003, pp. 669–679.

[18] Saumweber, C., Schulz, A., and Wittig, S., "Free-Stream Turbulence Effects on Film Cooling With Shaped Holes," *Journal of Turbomachinery*, Vol. 125, No. 1, 2003, pp. 65–72.

[19] Hale, C. A., Plesniak, M. W., and Ramadhyani, S., "Film Cooling Effectiveness for Short Film Cooling Holes Fed by a Narrow Plenum," *Journal of Turbomachinery*, Vol. 122, No. 3, 2000, pp. 553–557.

[20] Wilfert, G., and Wolff, S., "Influence of Internal Flow on Film Cooling Effectiveness," *Journal of Turbomachinery*, Vol. 122, No. 2, 2000, pp. 327–333.

[21] Gritsch, M., Schulz, A., and Wittig, S., "Effect of Internal Coolant Crossflow on the Effectiveness of Shape Film-Cooling Holes," *Journal of Turbomachinery*, Vol. 125, No. 3, 2003, pp. 547–554.

[22] Kohli, A., and Bogard, D. G., "Effects of Hole Shape on Film Cooling With Large Angle Injection," ASME Paper 99-GT-165, 1999.

[23] Sargison, J. E., Guo, S. M., Oldfield, M. L. G., Lock, G. D., and Rawlinson, A. J., "A Converging Slot-Hole Film-Cooling Geometry—Part 1: Low-Speed Flat-Plate Heat Transfer and Loss," *Journal of Turbomachinery*, Vol. 124, No. 3, 2002, pp. 453–460.

[24] York, W. D., and Leylek, J. H., "Leading-Edge Film-Cooling Physics —Part 3: Diffused Hole Effectiveness," *Journal of Turbomachinery*, Vol. 125, No. 2, 2003, pp. 252–259.

[25] Kim, Y. J., and Kim, S. M., "Influence of Shaped Injection Holes on Turbine Blade Leading Edge Film Cooling," *International Journal of Heat and Mass Transfer*, Vol. 47, No. 2, 2004, pp. 245–256.

[26] Bunker, R. S., "A Review of Shaped Hole Turbine Film-Cooling Technology," *Journal of Heat Transfer*, Vol. 127, No. 4, 2005, pp. 441–453.

[27] Immarigeon, A. A., "Advanced Impingement/Film-Cooling Schemes for High-Temperature Gas Turbine—Numerical Study," M.Sc. Thesis, Concordia Univ., Montreal, 2004.

[28] Sinha, A. K., Bogard, D. G., and Crawford, M. E., "Film-Cooling Effectiveness Downstream of a Single Row of Holes with Variable Density Ratio," *Journal of Turbomachinery*, Vol. 113, No. 3, 1991, pp. 442–449.

[29] Leylek, J. H., and Zerkle, R. D., "Discrete-Jet Film Cooling: A Comparison of Computational Results with Experiments," ASME

Paper 93-GT-207, 1993.
[30] Mulugeta, K. B., and Patankar, S. V., "A Numerical Study of Discrete-Hole Film Cooling," ASME Paper 96-WA/HT-8, 1996.
[31] Leitner, A., "Prediction of Three-Dimensional Film-Cooling Studies," Ph.D. Dissertation, Univ. of Minnesota, Minneapolis, MN, 1997.
[32] Ferguson, J. D., Walters, D. K., and Leylek, J. H., "Performance of Turbulence Models and Near-Wall Treatments in Discrete Jet Film Cooling Simulations," ASME Paper 98-GT-438, 1998.
[33] Walters, D. K., and Leylek, J. H., "A Detailed Analysis of Film Cooling Physics: Part 1: Streamwise Injection With Cylindrical Holes," *Journal of Turbomachinery*, Vol. 122, No. 1, 2000, pp. 102–112.
[34] Kapadia, S., and Roy, S., "Detached Eddy Simulation of Turbine Blade Cooling," AIAA Paper 2003-3632, 2003.
[35] Kim, S. W., and Benson, T. J., "Calculation of a Circular Jet in Crossflow with a Multiple-Time-Scale Turbulence Model," *International Journal of Heat and Mass Transfer*, Vol. 35, No. 10, 1992, pp. 2357–2365.
[36] Tyagi, M., and Acharya, S., "Large Eddy Simulation of Film Cooling Flow From an Inclined Cylindrical Jet," *Journal of Turbomachinery*, Vol. 125, No. 4, 2003, pp. 734–742.
[37] Hale, C. A., "An Experimental and Numerical Study of the Hydrodynamics and Surface Heat Transfer Associated with Short Film Cooling Holes Fed by a Narrow Plenum," Ph.D. Dissertation, Purdue Univ., West Lafayette, IN, 1999.
[38] Hoda, A., Acharya, S., and Tyagi, M., "Reynolds Stress Transport Model Predictions and Large Eddy Simulations for Film Coolant Jet in Crossflow," ASME Paper 2000-GT-249, 2000.
[39] Yu., Y., Yen, C. H., Shih, T. I. P., and Chyu, M. K., "Film Cooling Effectiveness and Heat Transfer Coefficient Distributions Around Diffusion Shaped Holes," *Journal of Heat Transfer*, Vol. 124, No. 5, 2002, pp. 820–827.
[40] Bell, C. M., Hamakawa, H., and Ligrani, P. M., "Film Cooling From Shaped Holes," *Journal of Heat Transfer*, Vol. 122, May 2000, pp. 224–
232.
[41] Taslim, M. E., and Khanicheh, A., "Film Effectiveness Downstream of a Row of Compound Angle Film Holes," *Journal of Heat Transfer*, Vol. 127, April 2005, pp. 434–440.